RECEIVER-COORDINATED DISTRIBUTED TRANSMIT BEAMFORMING WITH KINEMATIC TRACKING

D. Richard Brown III[*] *Patrick Bidigare*[†] *Upamanyu Madhow*[‡]

[*] Worcester Polytechnic Institute, 100 Institute Road, Worcester, MA 01609, drb@wpi.edu
[†] Raytheon BBN Technologies, 1300 17th Street Suite 400, Arlington, VA 22207, bidigare@ieee.org
[‡] University of California, Santa Barbara, CA 93106, madhow@ece.ucsb.edu

ABSTRACT

A distributed transmit beamforming technique is described for a scenario with two or more transmit nodes and one intended receiver. The protocol includes a measurement epoch, feedback from the intended receiver to the transmit nodes, and a beamforming epoch. The intended receiver tracks the clock and kinematic parameters of the independent transmit nodes and coordinates the transmit nodes by feeding back state predictions which are then used as phase corrections to facilitate passband phase and frequency alignment at the receiver. A three-state dynamic model is developed to describe the stochastic kinematics and clock evolution of each transmit node relative to the frame of the receiver/coordinator. Steady-state analysis techniques are used to analytically predict the tracking performance as well as the beamforming gain as a function of the system parameters. Numerical results show that near-ideal beamforming performance can be achieved if the period between successive observations at the receiver/coordinator is sufficiently small.

Index Terms— distributed beamforming, cooperative communication, feedback systems, oscillator dynamics, tracking

1. INTRODUCTION

Researchers have recently begun to consider the possibility of "distributed transmit beamforming" in which two or more *separate* information sources simultaneously transmit a common message and control the phase of their transmissions so that the signals constructively combine at an intended destination. Distributed transmit beamforming, sometimes also called "collaborative beamforming", is a powerful technique that offers the potential gains of conventional antenna arrays to wireless communication systems composed of multiple single-antenna transmitters with independent local clocks.

One of the key challenges of distributed transmit beamforming is aligning the phases of the transmit nodes' independent carriers such that their passband signals coherently combine at the intended destination. Several techniques have been proposed to enable distributed transmit beamforming including receiver-coordinated full-feedback [1], receiver-coordinated one-bit feedback [2, 3, 4], master-slave synchronization with retrodirective transmission [5], round-trip [6, 7], and two-way synchronization with retrodirective transmission [8, 9]. Distributed transmit beamforming has also been considered for the downlink of cellular networks under the title "coordinated multipoint" (CoMP), e.g. [10], which uses a received-coordinated full-feedback approach similar to [1]. Each of these techniques has advantages and disadvantages in particular applications, as discussed in the survey article [11].

Much of the prior work in this area has ignored the effects of stochastic clock drift and, with the exception of [7], the prior literature has also ignored the effects of node mobility. This paper describes a receiver-coordinated full-feedback distributed transmit beamforming technique within a state-space framework that includes the effects of stochastic clock drift and unpredictable kinematics. Our analysis also accounts for feedback latency, which can lead to stale channel state predictions and degraded performance. Steady-state analysis techniques are used to analytically predict the tracking performance as well as the beamforming gain as a function of the system parameters. Numerical results show that near-ideal beamforming performance can be achieved if the period between successive observations at the receiver/coordinator is sufficiently small.

2. SYSTEM MODEL

We consider the wireless communication system shown in Figure 1 with M transmit nodes and one receive node. The M transmit nodes are enumerated as nodes $1, \ldots, M$ and the receive node is denoted as node 0. Each node in the system is assumed to possess a single[1] isotropic antenna. Transmissions from the transmit nodes to the receiver are called "uplink" transmissions and feedback from the receiver to the transmit nodes occurs via the "downlink". The noise in each channel is assumed to be additive, white, and Gaussian.
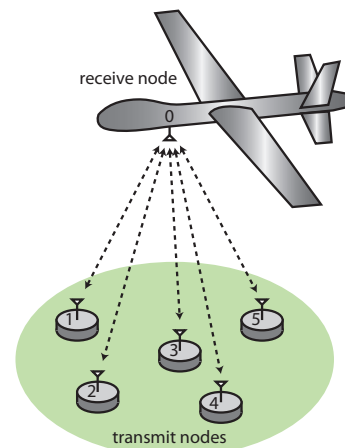

Fig. 1. System model example with $M = 5$ transmit nodes.

---

[1]Our focus on single antennas is motivated by clarity of exposition. The techniques developed in this paper can be extended to the case where nodes have more than one antenna at the expense of some additional notational complexity.

3. CLOCK AND KINEMATIC MODELING

In a conventional transmit beamformer, the transmit antennas are all driven by a common oscillator and typically remain in fixed relative positions. An important distinction in distributed transmit beamforming is that each transmit node has an independent local oscillator and may also move independently of the other transmit nodes. This section presents a state-space model for the independent clocks and kinematics of each transmit node relative to the frame of the receiver.

We define the discrete-time state of the ith transmit node's carrier as $\boldsymbol{x}^{(i)}[k] := [\phi^{(i)}[k], \dot{\phi}^{(i)}[k], \ddot{\phi}^{(i)}[k]]^{\top}$ where $\phi^{(i)}[k]$ corresponds to the *received carrier phase offset* in radians with respect to the carrier at the receive node at time k. Note that the state includes offsets due to independent clocks as well as kinematics and propagation from node i to the receive node. The state update of the ith node's received carrier offset is governed by

$$\boldsymbol{x}^{(i)}[k+1] = \begin{bmatrix} 1 & T_s & \frac{T_s^2}{2} \\ 0 & 1 & T_s \\ 0 & 0 & 1 \end{bmatrix} \boldsymbol{x}^{(i)}[k] + \boldsymbol{w}^{(i)}[k] \quad (1)$$

$$= \boldsymbol{F}\boldsymbol{x}^{(i)}[k] + \boldsymbol{w}^{(i)}[k] \quad (2)$$

where T_s is the sampling period and the process noise vector $\boldsymbol{w}^{(i)}[k] \overset{\text{i.i.d.}}{\sim} \mathcal{N}(0, \boldsymbol{Q}(T_s))$ includes the effect of clock and kinematic process noises that cause the carrier derived from the local oscillator at node i to deviate from the nominal carrier at the receive node. The process noise is assumed to be temporally white here for clarity of exposition. Our results can be straightforwardly extended to temporally correlated process noise via prewhitening and state-augmentation as discussed in [12, pp. 320-324].

At time k, if node i transmits an uplink signal to the receive node, the receive node directly downmixes the received signal with its own local carrier and measures the resulting phase difference according to the observation model

$$y^{(i)}[k] = \boldsymbol{H}\boldsymbol{x}^{(i)}[k] + v^{(i)}[k] \quad (3)$$

where $\boldsymbol{H} := [1, 0, 0]$ and $\boldsymbol{v}^{(i)}[k] \overset{\text{i.i.d.}}{\sim} \mathcal{N}(0, R)$ is the additive white Gaussian measurement noise in the observation.

3.1. Process Noise Covariance

In the absence of motion, a two-state model is typically sufficient for capturing the effect of the independent clocks [13, 14]. The covariance of the discrete-time clock process noise is given as $\boldsymbol{Q}_c(T_s) = \omega_c^2(q_1^2 \boldsymbol{V}_1(T_s) + q_2^2 \boldsymbol{V}_2(T_s))$ where

$$\boldsymbol{V}_1(T_s) := \begin{bmatrix} T_s & 0 & 0 \\ 0 & 0 & 0 \\ 0 & 0 & 0 \end{bmatrix} \qquad \boldsymbol{V}_2(T_s) := \begin{bmatrix} \frac{T_s^3}{3} & \frac{T_s^2}{2} & 0 \\ \frac{T_s^2}{2} & T_s & 0 \\ 0 & 0 & 0 \end{bmatrix}$$

and where the parameters q_1 (units of $\sec^{1/2}$) and q_2 (units of $\sec^{-1/2}$) can be estimated by fitting the theoretical Allan variance of the two-state model to experimental measurements of the Allan variance for a particular family of oscillators over a range of τ values. For example, the Allan variance specifications for a Rakon RFPO45 oven-controlled oscillator [15] yield a least squares fit of $q_1^2 = 5.39 \times 10^{-22}$ and $q_2^2 = 2.10 \times 10^{-23}$.

The covariance of the kinematic process noise depends on the application and can be obtained either by modeling or by empirical measurements. As an example, the piecewise constant white-jerk kinematic process noise model has a process noise given as [12]

$$\boldsymbol{Q}_k(T_s) = \omega_c^2(p_1^2 \boldsymbol{V}_1(T_s) + p_2^2 \boldsymbol{V}_2(T_s) + p_3^2 \boldsymbol{V}_3(T_s)) \text{ where}$$

$$\boldsymbol{V}_3(T_s) := \begin{bmatrix} \frac{T_s^5}{20} & \frac{T_s^4}{8} & \frac{T_s^3}{6} \\ \frac{T_s^4}{8} & \frac{T_s^3}{3} & \frac{T_s^2}{2} \\ \frac{T_s^3}{6} & \frac{T_s^2}{2} & T_s \end{bmatrix}$$

and where p_1 (units of $\sec^{1/2}$), p_2 (units of $\sec^{-1/2}$), and p_3 (units of $\sec^{-3/2}$) are process noise parameters corresponding to white frequency noise, integrated white frequency noise, and twice-integrated white frequency noise, respectively.

It is reasonable to assume the process noise due to node kinematics is independent of the clock process noise, hence

$$\boldsymbol{Q}(T_s) = \omega_c^2\Big((p_1^2 + q_1^2)\boldsymbol{V}_1(T_s) + (p_2^2 + q_2^2)\boldsymbol{V}_2(T_s) + p_3^2\boldsymbol{V}_3(T_s)\Big).$$

4. RECEIVER-COORDINATED DISTRIBUTED TRANSMIT BEAMFORMING PROTOCOL

An overview of the receiver-coordinated distributed transmit beamforming protocol is shown in Figure 2. Uplink transmissions are divided into measurement and beamforming epochs, repeating periodically with period T_m. Downlink transmissions provide feedback from the receive node to the transmit nodes and are assumed to be on a different frequency than the uplink signals. Note that the protocol includes the effects of feedback latency.
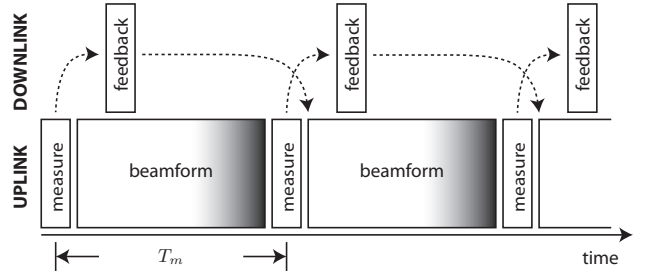

Fig. 2. Receiver-coordinated distributed transmit beamforming.

During the uplink measurement epochs, the transmit nodes simultaneously transmit using code division multiple access to facilitate signal separation at the receive node. We assume that the frequency offsets are small with respect to the duration of the measurement such that the phase of the received signal is approximately constant during the measurement epoch. The receive node estimates the phase of the received signal from each transmit node, resulting in noisy phase observations for each transmit node according to (3). These observations are then provided to a Kalman filter to generate state estimates $\hat{\boldsymbol{x}}^{(i)}[k|k]$ and state predictions $\hat{\boldsymbol{x}}^{(i)}[k+L|k]$ for the start of the next beamforming epoch, for each node $i = 1, \ldots, M$. The value of L is equal to the product of the feedback latency, i.e. the time between the observation and the start of the beamforming epoch in which the observation is used, and the sampling frequency.

The feedback from the receive node to transmit node i is its state prediction vector for the start of the next beamforming epoch, i.e. $\hat{\boldsymbol{x}}^{(i)}[k+L|k]$. Over the beamforming epoch, each node uses its state prediction vector to compute a *corrected* transmit phase so that the phase offset at the receive node is nominally zero. For example, if the feedback $\hat{\boldsymbol{x}}^{(1)}[k+L|k] = [\pi/2, -2\pi/1000]^{\top}$, transmit node 1

will apply a phase correction of $-\pi/2$ at the start of the beamforming epoch and a frequency correction of $-2\pi/1000$ over the duration of the beamforming epoch. Since each transmit node corrects its phase and frequency offsets according to the state predictions fed back from the receive node, the signals combine coherently at the receive node and the nodes operate as a distributed beamformer.

5. STEADY-STATE BEAMFORMING POWER ANALYSIS

This section analyzes the steady-state performance of the receiver-coordinated distributed transmit beamforming system. We first present a useful received power approximation that can be applied when the phase offsets of each node are independent and identically distributed (i.i.d). We then use steady-state analysis techniques to compute the Kalman filter's prediction covariance during the beamforming epoch.

5.1. Received Power Approximation

During the beamforming epoch, assuming unit gain channels, the mean received power can be written as

$$\rho[k] = \mathrm{E}\left\{\left|\sum_{i=1}^{M} e^{j\phi^{(i)}[k]}\right|^2\right\}$$

$$= \mathrm{E}\left\{\left(\sum_{i=1}^{M}\cos(\phi^{(i)}[k])\right)^2\right\} + \mathrm{E}\left\{\left(\sum_{i=1}^{M}\sin(\phi^{(i)}[k])\right)^2\right\}$$

$$= \mathrm{E}\left\{C^2\right\} + \mathrm{E}\left\{S^2\right\}$$

where $\phi^{(i)}[k]$ corresponds to the first element of the state vector $\boldsymbol{x}^{(i)}[k]$. Note that $\phi^{(i)}[k]$ is a zero-mean Gaussian random variable at time k. Although $\cos(\phi^{(i)}[k])$ and $\sin(\phi^{(i)}[k])$ are not Gaussian distributed, if we assume that the $\phi^{(i)}[k]$ are i.i.d. at time k with zero mean and variance $\sigma_\phi^2[k]$, the central limit theorem implies that the sums C and S will be approximately Gaussian when M is reasonably large. It can be shown through straightforward integration that

$$\mathrm{E}\left\{\cos(\phi^{(i)}[k])\right\} = \exp(-\sigma_\phi^2[k]/2)$$
$$\mathrm{E}\left\{\sin(\phi^{(i)}[k])\right\} = 0$$
$$\mathrm{var}\left\{\cos(\phi^{(i)}[k])\right\} = \frac{1}{2}\left(1 - \exp(-\sigma_\phi^2[k])\right)^2$$
$$\mathrm{var}\left\{\sin(\phi^{(i)}[k])\right\} = \frac{1}{2}\left(1 - \exp(-2\sigma_\phi^2[k])\right).$$

Applying the central limit theorem, we have

$$C \sim \mathcal{N}\left(M\exp(-\sigma_\phi^2[k]/2), \frac{M}{2}\left(1 - \exp(-\sigma_\phi^2[k])\right)^2\right)$$
$$S \sim \mathcal{N}\left(0, \frac{M}{2}\left(1 - \exp(-2\sigma_\phi^2[k])\right)\right).$$

Hence,

$$\mathrm{E}\left\{C^2\right\} + \mathrm{E}\left\{S^2\right\} = \mathrm{E}\{C\}^2 + \mathrm{E}\{S\}^2 + \mathrm{var}\{C\} + \mathrm{var}\{S\}$$
$$= M^2\exp(-\sigma_\phi^2[k]) + M\left(1 - \exp(-\sigma_\phi^2[k])\right).$$

This intuitively satisfying result shows that the beamforming power at the receiver is a convex combination of the ideal coherent beamforming power M^2 and the non-coherent power M. In the absence of phase errors, the received power is that of an ideal beamformer

M^2. With very large phase error variance, the received power approaches the incoherent lower bound of M. As shown in Figure 3, this result is also surprisingly accurate even for small values of M. The next section shows how the phase error variance $\sigma_\phi^2[k]$ can be computed through steady-state analysis techniques.
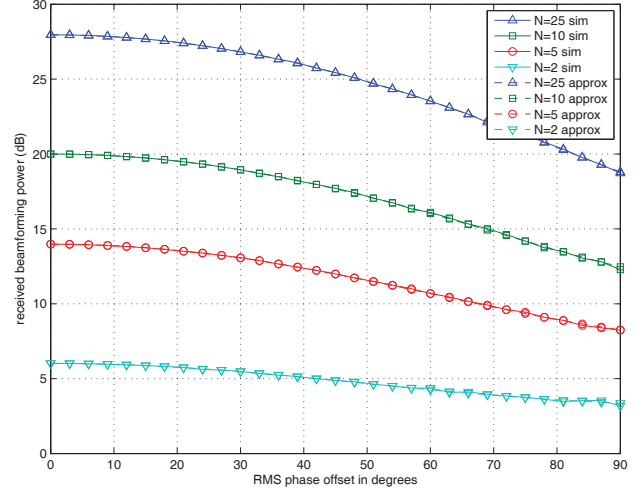

Fig. 3. Received beamforming power as a function of $\sigma_\phi[k]$. Note the close correspondence between the approximation and the simulated results.

5.2. Steady-State State Prediction Error Covariance

Referring back to the discrete-time model presented in Section 3, note that the pair $\{\boldsymbol{F}, \boldsymbol{H}\}$ is completely observable. Denoting $\boldsymbol{Q}(T_m) = \boldsymbol{C}^\top(T_m)\boldsymbol{C}(T_m)$ and assuming the pair $\{\boldsymbol{F}, \boldsymbol{C}(T_m)\}$ is completely observable, then the steady-state prediction covariance is a unique positive definite matrix specified as the solution to the discrete-time algebraic Riccati equation [12]

$$\boldsymbol{P} = \boldsymbol{F}(T_m)\left[\boldsymbol{P} - \frac{\boldsymbol{P}\boldsymbol{H}^\top\boldsymbol{H}\boldsymbol{P}}{\boldsymbol{H}\boldsymbol{P}\boldsymbol{H}^\top + R}\right]\boldsymbol{F}(T_m)^\top + \boldsymbol{Q}(T_m).$$

Note that this steady-state prediction covariance corresponds to the covariance of the state prediction just prior to an observation. The steady-state estimation covariance (immediately after an observation) is then

$$\boldsymbol{S} = \boldsymbol{P} - \frac{\boldsymbol{P}\boldsymbol{H}^\top\boldsymbol{H}\boldsymbol{P}}{\boldsymbol{H}\boldsymbol{P}\boldsymbol{H}^\top + R}. \tag{4}$$

To predict the performance of the receiver-coordinated distributed transmit beamforming system, it is necessary to compute the covariance of the state predictions during the beamforming epochs. To do this, we project the steady-state estimation covariance forward to samples in the beamforming epoch at elapsed time $dt \in [t_1, t_2)$, where t_1 and t_2 correspond to the feedback latency from the observation to the start and end of the beamforming epoch, respectively, from the kth observation by computing

$$\boldsymbol{P}(dt\,|\,k) = \boldsymbol{F}(dt)\boldsymbol{S}\boldsymbol{F}^\top(dt) + \boldsymbol{Q}(dt). \tag{5}$$

The (1,1) element of this result corresponds to $\sigma_\phi^2[k]$ and can be substituted into the received power approximation developed in the previous section to compute the steady-state mean beamforming power at any point during the beamforming epoch.

6. NUMERICAL RESULTS

Figure 4 shows an example of the mean received power of the receiver-coordinated distributed beamforming system for a case with 10 transmit nodes transmitting at 900MHz, a measurement epoch 2ms with measurements taken every $T_m = 250$ms, and a feedback latency of 100ms. The process noise parameters were set to $\omega_c^2(q_1^2 + p_1^2) = 3.4 \times 10^{-4}$, $\omega_c^2(q_2^2 + p_2^2) = 0.58$, and $\omega_c^2 p_3^2 = 1.00$. The standard deviation of the phase measurement error at the receive node was set to 5 degrees.
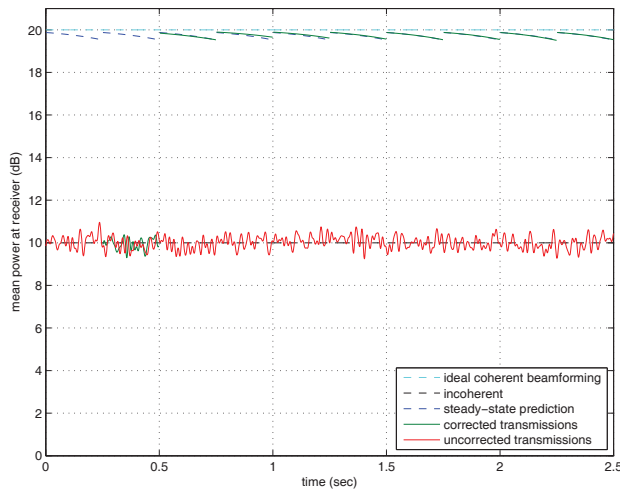

Fig. 4. Mean received power of the receiver-coordinated distributed beamforming system for a case with 10 transmit nodes.

These results show that near ideal beamforming is achieved by the receiver coordinated distributed beamforming system in the third and subsequent beamforming epochs. In the first beamforming epoch, the nodes do not transmit because they do not have feedback in time to correct their phases (recall that the feedback has 100ms of latency). The nodes do transmit in the second beamforming epoch, but the frequency estimates are so poor that the signals combine incoherently at the receiver. In the third beamforming epoch (from 0.502s to 0.750s), coherent combining is achieved. This is because the phase and frequency predictions from the Kalman filter are now good enough to accurately correct the transmission phases of the nodes so that the passband signals arrive nearly in phase at the receiver. In fact, the Kalman filters have approximately achieved their steady-state prediction in the third beamforming epoch. The beamforming gain remains within 0.5dB of ideal over the duration of the beamforming epoch.

7. CONCLUSIONS

This paper describes a receiver-coordinated full-feedback distributed transmit beamforming technique that includes the effects of stochastic clock drift and unpredictable kinematics. Steady-state analysis techniques are used to analytically predict the tracking performance as well as the beamforming gain as a function of the system parameters. Numerical results show that near-ideal beamforming performance can be achieved.

8. REFERENCES

[1] Y.S. Tu and G.J. Pottie, "Coherent cooperative transmission from multiple adjacent antennas to a distant stationary antenna through AWGN channels," in *IEEE Vehic. Techn. Conf. (VTC)*, Birmingham, AL, Spring 2002, vol. 1, pp. 130–134.

[2] R. Mudumbai, J. Hespanha, U. Madhow, and G. Barriac, "Scalable feedback control for distributed beamforming in sensor networks," in *IEEE Int. Symp. on Information Theory (ISIT)*, Adelaide, Australia, September 2005, pp. 137–141.

[3] R. Mudumbai, B. Wild, U. Madhow, and K. Ramchandran, "Distributed beamforming using 1 bit feedback: from concept to realization," in *44th Allerton Conf. on Comm., Control, and Computing*, Monticello, IL, Sep. 2006, pp. 1020 – 1027.

[4] R. Mudumbai, J. Hespanha, U. Madhow, and G. Barriac, "Distributed transmit beamforming using feedback control," *IEEE Trans. on Information Theory*, vol. 56, no. 1, pp. 411–426, January 2010.

[5] R. Mudumbai, G. Barriac, and U. Madhow, "On the feasibility of distributed beamforming in wireless networks," *IEEE Trans. on Wireless Communications*, vol. 6, no. 5, pp. 1754–1763, May 2007.

[6] Ipek Ozil and D.R. Brown III, "Time-slotted round-trip carrier synchronization," in *Proceedings of the 41st Asilomar Conference on Signals, Systems, and Computers*, Pacific Grove, CA, November 4-7, 2007, pp. 1781 – 1785.

[7] D.R. Brown III and H.V. Poor, "Time-slotted round-trip carrier synchronization for distributed beamforming," *IEEE Trans. on Signal Processing*, vol. 56, no. 11, pp. 5630–5643, November 2008.

[8] R.D. Preuss and D.R. Brown, "Retrodirective distributed transmit beamforming with two-way source synchronization," in *Information Sciences and Systems (CISS), 2010 44th Annual Conference on*, march 2010, pp. 1 –6.

[9] R. Preuss and D.R. Brown III, "Two-way synchronization for coordinated multi-cell retrodirective downlink beamforming," *IEEE Trans. on Signal Processing*, November Accepted to appear in 2011.

[10] R. Irmer, H. Droste, P. Marsch, M. Grieger, G. Fettweis, S. Brueck, H.-P. Mayer, L. Thiele, and V. Jungnickel, "Coordinated multipoint: Concepts, performance, and field trial results," *Communications Magazine, IEEE*, vol. 49, no. 2, pp. 102–111, february 2011.

[11] R. Mudumbai, D.R. Brown III, U. Madhow, and H.V. Poor, "Distributed transmit beamforming: Challenges and recent progress," *IEEE Communications Magazine*, vol. 47, no. 2, pp. 102–110, February 2009.

[12] Yaakov Bar-Shalom, X. Rong Li, and Thiagalingam Kirubarajan, *Estimation with Applications to Tracking and Navigation*, John Wiley and Sons, 2001.

[13] C. Zucca and P. Tavella, "The clock model and its relationship with the allan and related variances," *Ultrasonics, Ferroelectrics and Frequency Control, IEEE Transactions on*, vol. 52, no. 2, pp. 289 –296, feb. 2005.

[14] Lorenzo Galleani, "A tutorial on the two-state model of the atomic clock noise," *Metrologia*, vol. 45, no. 6, pp. S175–S182, December 2008.

[15] "Rakon RFPO45 SMD oven controlled crystal oscillator datasheet," 2009.